PHYSICAL REVIEW B VOLUME 3, NUMBER 2 15 JANUARY 1971

Normal-Incidence Reflectance, Optical Properties, and Electronic Structure of Zn†

G. W. Rubloff*‡
Department of Physics, The University of Chicago, Chicago, Illinois 60637
(Received 5 August 1970)

The normal-incidence reflectance of electropolished Zn single crystals has been measured from 0.6 to 4.0 eV at 300 and 77 °K for the polarization vector $\vec{E}$ parallel and perpendicular to the crystallographic $\vec{c}$ axis. Optical constants are determined through Kramers-Kronig inversion using a free-electron-like extrapolation for the reflectance outside the range of measurement. Results for ϵ_2/λ are compared with optical spectra recently calculated by Kasowski using the band-structure calculation of Stark and Falicov, in which the coefficients of a nonlocal pseudopotential were adjusted to fit the band structure to Fermi-surface data. The present optical data agree with theory much better than do previous oblique incidence reflectance data. As predicted by the theory, a structure in ϵ_2/λ at 0.9 eV arising from transitions along ΓM and ΓK and allowed only for $\vec{E} \parallel \vec{c}$ is observed with good agreement in shape and position in energy. For both polarizations a double peak around 1.6–2.1 eV is seen; its shape agrees well with a double peak around 2.2–2.9 eV predicted for transitions along LH in the Brillouin zone. The discrepancy in energy can be partly understood in terms of the limited accuracy of the pseudopotential and of the fit to Fermi-surface data. Application of the sum rule to the experimental ϵ_2/λ gives $n_{eff} \approx 2$ for both polarizations, which indicates that the extrapolation procedure used for Kramers-Kronig analysis and the magnitudes of interband structures in ϵ_2/λ obtained from experiment are reasonable. In contrast, n_{eff} calculated from theory suggests that the interband matrix elements are at least 10–20% too large. Temperature dependence is also discussed.

I. INTRODUCTION

Pseudopotential band structures have been calculated for many crystals.[1] In semiconductors the pseudopotential coefficients are usually adjusted to give optical gaps and cyclotron masses in agreement with experiment at symmetry points in the Brillouin zone. In metals the pseudopotential coefficients can also be determined by comparison with Fermi-surface data. These band structures, accurate at the Fermi energy E_F, can then be used to calculate the optical spectrum. Because optical absorption involves electronic states both below and above E_F, the comparison of the calculated and measured optical spectra tests the accuracy of these one-electron band structures at energies away from E_F.

This kind of comparison has been made in several types of metals, including simple metals, e.g., Na[2] and Al,[3] and noble metals, e.g., Cu.[4] In Na and Al and in Cu above 4 eV there was good agreement between experiment and theory in regard to position and shape of structure in the optical spectrum. In Cu the problem is greatly complicated by the mixing of the d bands into the conduction bands. In all three cases the calculations involved only local pseudopotentials.

Stark and Falicov[5] (SF) have calculated the band structure of Zn by adjusting the pseudopotential coefficients to achieve good agreement with Fermi-surface data; this required the use of a strongly nonlocal pseudopotential. The band structure of Zn should be simpler to calculate and more accurate than that of Cu because the d bands lie below the bottom of the conduction bands. Thus the conduction bands originate from the two s electrons in the valence shell of the free atom. The conduction-band wave functions are formed from free-electron eigenstates orthogonalized to the d core states just below the conduction bands. In the pseudopotential scheme these orthogonalization terms, large because of the relatively small energy (a few eV) between the bottom of the conduction bands and the d bands, produce a strong, nonlocal, d-like contribution to the pseudopotential. The simplicity of the basis functions in Zn compared to the s-d admixture in Cu suggests that the optical spectrum calculated from the band structure of Zn should be at least as accurate as that for Cu and nearly as good as that for the simple metals.

Kasowski[6] used the SF band structure to calculate the interband optical spectra of Zn, ignoring spin-orbit coupling. For comparison, at low photon energies (infrared-visible) two sets of experiments exist for Zn, both using a modified Drude technique for oblique incidence reflectance. The work by Graves and Lenham[7] (GL) was performed at 298 and 77 °K on hand polished samples, while Lettington[8] obtained similar results with electropolished samples at room temperature.

The experimental results of GL and the theoretical results of Kasowski are shown in Fig. 1. The measured optical structures are not in good agreement with the theory; no clear correlation between experimental and theoretical structures is possible. Furthermore, Kasowski's assignment of optical

structure to regions of the Brillouin zone is not consistent with the observed differences in the shape of structures appearing for the two polarizations. A more detailed discussion of these points will follow. But one should certainly expect better agreement between theory and experiment.

Oxide layers and surface films are often a problem in the preparation of good single-crystal surfaces of metals. The oblique incidence reflectance methods used in prior experiments on Zn are considerably more sensitive to these surface problems than is normal incidence reflectance. On the other hand, the optical constants cannot be determined directly from normal incidence reflectance, but must be obtained through a Kramers-Kronig inversion involving extrapolations of the reflectance into unmeasured regions of the spectrum.[9] However, the shape and position of structure are quite insensitive to the details of the extrapolations. The magnitudes of the optical constants can be partially corrected by invoking sum rules to choose proper extrapolations.

This paper reports normal incidence reflectance data for Zn between 0.6 and 4.0 eV carried out at 300 and 77 °K, with optical constants determined from the data by Kramers-Kronig analysis. The purpose of this work is (a) to check the previous experimental results by an independent experiment and technique; (b) to compare the new results with the calculations of Kasowski; (c) to analyze the experimental spectra in terms of the band structure; and (d) to attempt to determine the success of the SF empirical nonlocal pseudopotential band structure of Zn, calibrated at E_F, in predicting electronic eigenvalues away from E_F as seen in optical absorption.

II. EXPERIMENTAL TECHNIQUE

A high-precision normal incidence scanning reflectometer[10] was used to record the reflectance R directly as the photon energy $\hbar\omega$ was scanned. A quartz light pipe, bent slightly off axis at the top, captures both the incident (I_0) and the reflected (RI_0) beams in alternate positions; the off-axis bend allows the incoming beam to pass by the light pipe and strike the sample at near-normal (≈ 6°) incidence when the reflected beam is being captured. In this way a single detector and essentially the same optical path are used for both beams. The light pipe is rotated at about 70 Hz. Each beam contributes to the signal a flat pulse about 20% of the rotational period wide. The signal is processed by an electronic gating circuit which extracts the average height of each of the two pulses. The incident beam signal controls the detector gain to keep the magnitude of the incident beam signal constant. The reflected beam then yields a direct reading of the reflectance as the photon energy is scanned.

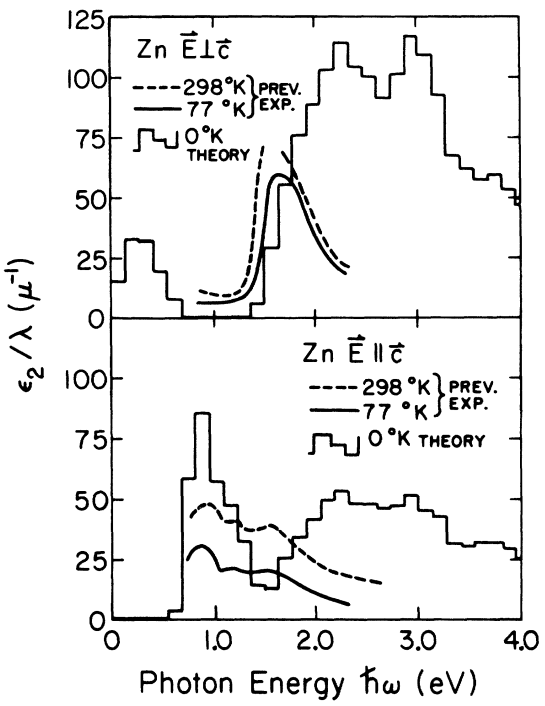

FIG. 1. Optical constants of Zn. Previous experiment from Graves and Lenham (Ref. 7), theory from Kasowski (Ref. 6).

In the visible and ultraviolet a photomultiplier is used as a detector, while at photon energies below 1.5 eV, the cutoff of the photomultiplier, a PbS cell with a 1-cm^2 area is used. Additional channels measure the signal during parts of the rotational period when neither beam is captured by the light pipe. Thus the dark current of the photomultiplier (or dark resistance of the PbS cell) is automatically subtracted from both I_0 and RI_0 to give a true reading of the reflectance. With the PbS cell the relative error in R is $\pm 5\times10^{-4}$, while with the photomultiplier it is $\pm 10^{-4}$.

Single crystals of Zn were grown by zone melting and oriented by Laue back-reflection techniques. Samples were spark cut with surfaces parallel to the $\vec{c}$ axis. Thus the reflectance for both $\vec{E}\parallel\vec{c}$ and $\vec{E}\perp\vec{c}$ could be measured for the same surface by simply rotating the plane of polarization of the incoming light. The samples were chemically etched in HNO_3, then electropolished in a 1:1 phosphoric acid and ethanol solution, and finally rinsed with fresh methanol. A rinse in distilled de-ionized water or even the presence of excess water in the methanol tends to create a bluish cast on the surface. This effect is attributed to the adhering of $(OH)^-$ radicals to the surface,[11] because when the polarity of the electrodes in the electropolish is reversed briefly to make Zn the cathode, this cast

disappears. Consequently, care was taken to keep the samples as free of water as possible.

The samples were mounted in a stainless-steel cryostat which was evacuated to better than 10^{-1} Torr by a liquid-nitrogen-trapped oil diffusion pump. The samples were thermally connected to a liquid-nitrogen trap inside the cryostat by a stainless-steel holder which allowed them to cool in about 1 h. Hence the residual gas in the chamber was cryopumped by the trap before the sample surface was cold. The samples were located directly behind a quartz window, which was tilted with respect to the sample by a small angle. In this manner the cryostat could be adjusted in such a way that the reflections from the window were not captured by the light pipe, and the correction for the window reflections could be straightforwardly computed. In this configuration the absolute error in R is about $\pm 2\%$, independent of photon energy.

Measurements of reflectance were made in the range 0.6–4.0 eV at 300 and 77 °K using a prism monochromator and triple-reflection polarizer of better than 97% efficiency. Two sets of measurements were made on the samples, one with a PbS cell and tungsten lamp, and the other with a photomultiplier and high-pressure xenon lamp. The two sets overlap in energy, and a vertical shift of less than 3% in reflectance was sufficient to match the two sets of curves in the overlap region.

III. REFLECTANCE DATA

The normal incidence reflectance spectra of Zn from 0.5 to 3.0 eV at 300 and 77 °K are shown in Fig. 2. The actual measurements begin at 0.6 eV; below this energy the curves are extrapolated to a constant reflectance close to 100% in accordance with the expected Drude behavior. Such an extrapolation, carried to zero energy, is used for the Kramers-Kronig analysis, which is to be discussed later. Its validity is experimentally indicated by the apparent saturation of the measured reflectance near 100% as $\hbar\omega \to 0.7$ eV from higher energies. Measurements were carried out to 4.0 eV in the ultraviolet; they showed a slight smooth decrease in reflectance with increasing photon energy. We attribute this decrease to the presence of an oxide layer on the sample surface.

Structure in the reflectance spectra of Zn is contained in a band of energies from 0.6 to 2.6 eV. In the absence of interband absorption, the reflectance would have the Drude shape: R large and nearly constant up to the plasma energy $\hbar\omega_p \approx 10$ eV and then dropping to very small values above $\hbar\omega_p$. Thus the departure of the measured spectrum from the drude shape must be attributed to interband absorption, which yields structure concentrated primarily in the range 0.6–2.6 eV.

The major anisotropy in the spectra is the peak at 1.0 eV, which occurs only for $\vec{E} \parallel \vec{c}$. It appears to suppress the sharp drop in reflectance seen for $\vec{E} \perp \vec{c}$ near 1 eV. At 77 °K the peak sharpens considerably and shifts to lower energy.

Shoulders occur at 1.6 and 2.3 eV for both polarizations and sharpen at lower temperature. An additional shoulder appears at 1.3 eV for $\vec{E} \perp \vec{c}$ and for $\vec{E} \parallel \vec{c}$ at 77 °K superimposed on the high-energy side of the main anisotropic peak. Weak shoulders were also noted for both polarizations in the region where the reflectance drops from nearly 100%, i.e., at the onset of interband absorption.

A 7% decrease in reflectance near 3 eV is evident for $\vec{E} \perp \vec{c}$ upon cooling to 77 °K while for $\vec{E} \parallel \vec{c}$ the reflectance remains constant within the absolute error. This polarization-dependent change in reflectance with temperature is puzzling and its cause is not understood. The high-vacuum conditions of the experiment should rule out condensed gases on the surface at low temperatures, particularly for such low photon energies. Furthermore, one would expect such condensation to produce a decrease in reflectance for both polarizations, but no temperature shift is observed for $\vec{E} \parallel \vec{c}$.

Independent evidence for a temperature shift for $\vec{E} \perp \vec{c}$ ($\vec{E} \parallel \vec{c}$ could not be measured) is found in the photoemission data of Mosteller, Huen, and Wooten.[12] In their results, the magnitude of the photoelectron energy distribution $N(E)$ in the ultraviolet for Zn basal-plane surfaces cleaved in vacuum decreased by about 10% as the temperature

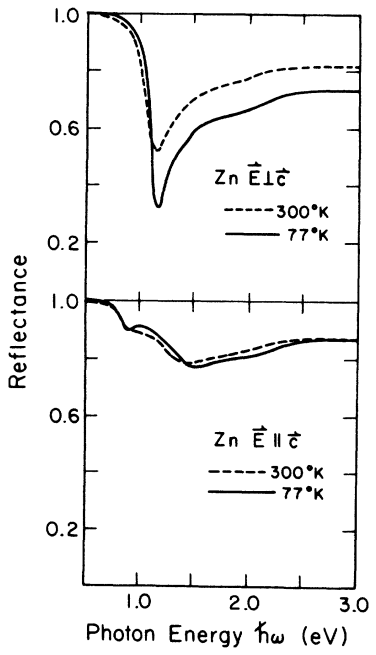

FIG. 2. Normal incidence reflectance of Zn.

was reduced from 290 to 96 °K. They suggest that this decrease might be attributed to a change in the optical absorption coefficient with temperature. In our case, the samples were exposed to air before being measured, so that we cannot exlude the possibility of a polarization-dependent change in the absorption coefficient with temperature for the oxide layer at the surface. Although the effect is still unexplained, it does not significantly affect the determination of the position and shape of structure in the optical spectra, which is the main contribution of this work.

IV. KRAMERS-KRONIG ANALYSIS

The optical constants are determined from normal incidence reflectance by applying the Kramers-Kronig relations to the complex reflectance to obtain the phase shift Θ on reflection. Because $\Theta(\omega_0)$ depends on the reflectance $R(\omega)$ for all ω, the extrapolation of the reflectance at both ends of the spectrum is crucial. Extrapolating R to $\approx 100\%$ at low energy, as mentioned in the previous section, appears very reasonable. The high-energy extrapolation requires further discussion.

The measured reflectance of Zn shows a gradual decrease ($\approx -3\%$/eV) in R above 2.6 eV as $\hbar\omega$ increases. We attribute most of this decrease to the existance of an oxide layer on the Zn surface. The effect of the oxide should become more serious at larger photon energies. Therefore we suspect that the high-energy limit of our measurements does not represent the reflectance purely of the bulk Zn. Additional experimental information is needed to make a reasonable high-energy extrapolation of the reflectance.

Mosteller and Wooten[13] have found the reflectance of clean vacuum-cleaved Zn in the ultraviolet to be similar to the reflectance calculated from the free-electron dielectric functions

$$\epsilon_1(\omega) = 1 - \frac{\omega_p^2}{\omega^2 + 1/\tau^2} \quad , \tag{1}$$

$$\epsilon_2(\omega) = \frac{\omega_p^2}{\omega\tau(\omega^2 + 1/\tau^2)} \quad , \tag{2}$$

with a plasma energy $\hbar\omega_p = 10.1$ eV and a relaxation time $\tau \approx 2\times 10^{-15}$ sec. This reflectance is nearly constant from 2.2 to 6.5 eV. They found that when the sample is exposed to air, the reflectance in this energy range decreases, similar to our results.

Mosteller and Wooten could only measure the reflectance for $\vec{E} \perp \vec{c}$ since Zn cleaves in the basal plane. The reflectance curves for $\vec{E} \parallel \vec{c}$ and $\vec{E} \perp \vec{c}$ should have the same shape above 2.6 eV if they are free-electron-like. We performed measurements on both polarizations with the scanning reflectometer using as a light source in the vacuum uv the polarized synchrotron radiation from the 240-MeV electron storage ring at the University of Wisconsin. No polarization dependence was detected in the shape or position of the plasma edge. Futhermore, the shape of the reflectance was that found by Mosteller and Wooten for slightly oxidized surfaces, which is reasonable since our samples were chemically etched and put into vacuum within 10 min of removal from the etch.

The reflectance values of Mosteller and Wooten are larger than our values near 3.0 eV. Thus, joining our curves to their values would introduce artificial structure in the optical constants, which is unacceptable. In order to generate a free-electron-like extrapolation of our reflectance curves without introducing artificial structure, we calculated the reflectance from Eqs. (1) and (2) with $\hbar\omega_p = 10.1$ eV and $\tau = 10^{-15}$ sec, and multiplied these reflectances by a scale factor[14] to match the measured curves smoothly near 3.0 eV. In this way the shape and position of the interband structure at lower energies remains unaltered.

Changing the value of τ from 10^{-15} to 3×10^{-15} sec in the calculation results in no shift of the position of the ϵ_2/λ structure and an increase in magnitude by less than $\frac{1}{2}\%$. Hence the choice of τ is not critical, and $\tau = 10^{-15}$ sec was used in all extrapolations because this value yields the best fit to the slope of the measured reflectance at the matching point near 3 eV. The value of $\hbar\omega_p$ is well established and could not be used as an adjustable parameter. On the other hand, if the actual measurements showing the decrease in reflectance above 3.0 eV are used and extrapolated smoothly to an edge at $\hbar\omega_p$, the position of the double peak in ϵ_2/λ shifts to lower energy by as much as 0.2 eV and the magnitudes decrease by a factor of between 3 and 4. This yields unreasonably low values for the sum rule discussed below.

The use of a single relaxation time for both polarizations and different temperatures is a simplification which masks changes in τ by a factor of 2 or 3 as indicated by the anisotropy and temperature dependence of electrical conductivity. The changes in ϵ_2/λ from such a variation in τ are small, as discussed above. This means that the decrease in reflectance with temperature for $\vec{E} \perp \vec{c}$ cannot be attributed to the temperature dependence of τ.

V. OPTICAL CONSTANTS: COMPARISON WITH THEORY AND PREVIOUS EXPERIMENT

The "optical conductivity" $\epsilon_2/\lambda = 2nk/\lambda$ derived from Kramers-Kronig analysis of reflectance measurements for Zn is shown in Fig. 3. The interband optical spectrum calculated by Kasowski is also shown. These results are to be compared with previous measurements shown in Fig. 1.

The intraband or free-carrier contribution to

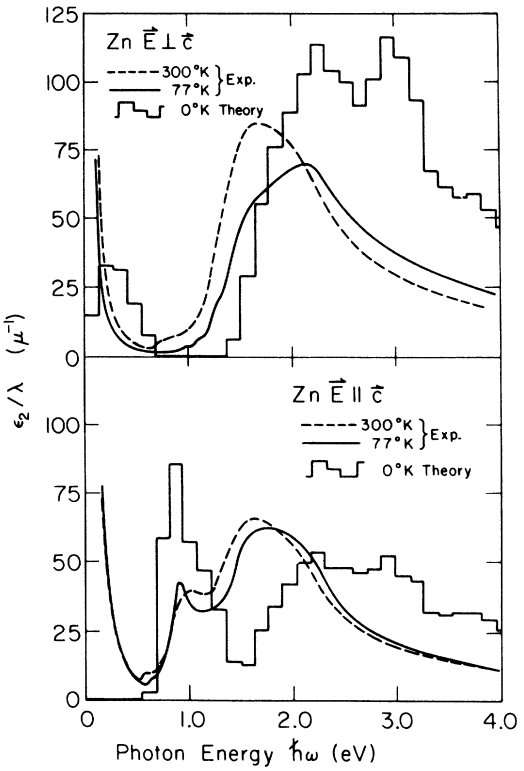

FIG. 3. Optical constants of Zn. Theory from Kasowski (Ref. 6).

ϵ_2 is given by Eq. (2). Thus $(\epsilon_2/\lambda)_{\text{intra}}$ due to free carriers is proportional to $1/\omega^2$, except at very small photon energies for which $\omega \ll 1/\tau$ and $(\epsilon_2/\lambda)_{\text{intra}}$ becomes large and constant. The intraband portion of ϵ_2/λ is seen below 0.5 eV in Fig. 3. Since ϵ_2/λ drops to small values near 0.5 eV, the structure above this energy can be considered essentially all interband absorption.

The reflectance peak at 1.0 eV for $\vec{E} \parallel \vec{c}$ gives rise to the peak in ϵ_2/λ near 0.9 eV, which sharpens and shifts to lower energy with decreasing temperature. The sign of the temperature shift is somewhat unusual but in agreement with the GL results. This peak is in excellent agreement with the theory in regard to position and shape. The asymmetry of the peak, i.e., sharper on the low-energy side, is clearly reproduced in the theory, whereas this feature is not obvious in the GL results. The magnitudes are in disagreement by a factor of 2.

The calculated peak for $\vec{E} \perp \vec{c}$ at 0.25 eV is not expected to appear in the present results because the lower limit of these measurements was 0.6 eV. Other experimental techniques, e.g., calorimetry, may be preferable at photon energies below the quartz infrared cutoff unless a better infrared-transmitting material is used for the light pipe.

Broad peaks in ϵ_2/λ occur for both polarizations near 1.6 eV. They show an additional shoulder on the high-energy side near 2.1 eV. The shape and location of this structure is similar for all four curves, except that the relative height of the peak and shoulder reverses for $\vec{E} \perp \vec{c}$ at 77 °K. (This may arise from the temperature dependence of the reflectance magnitude.) Comparison with the theory suggests that this structure is to be associated with the broad double peak arising for both polarizations and centered at 2.5 eV. The half-width of this structure is about 1 eV in both experiment and theory. The positions in energy disagree by about 0.9 eV. Furthermore, this doublet seems more clearly resolved in the calculation than in the experiment. The discrepancy in energy location is too large to be explained by the fact that the calculations are based on He-temperature data, whereas the optical experiments are carried out at much higher temperatures, even though the temperature shift measured experimentally is in the right direction.

This experimental double peak in ϵ_2/λ at 1.6–2.1 eV is similar to the GL result for $\vec{E} \perp \vec{c}$. The GL structure for $\vec{E} \parallel \vec{c}$ at 1.6 eV is very different, however. Thus our normal incidence results differ from the oblique incidence measurements of GL (and also those of Lettington) primarily for $\vec{E} \parallel \vec{c}$. We see no evidence of the middle peak which appears in their data and which is also absent in the theoretical results of Kasowski. Furthermore, we do not observe the large decrease in ϵ_2/λ upon cooling found by GL for $\vec{E} \parallel \vec{c}$.

The present measurements provide improved agreement between theory and experiment for the shape of the interband optical spectra of Zn. This fact generates increased confidence in the accuracy of the SF band structure away from the Fermi energy, but also emphasizes the need to understand the error in the energy position of the double peak.

VI. DISCUSSION

The SF band structure of Zn is shown in Fig. 4. The notation of the single group is used because the optical spectra were calculated ignoring spin-orbit interactions. For reference the first Brillouin zone for the hexagonal close-packed lattice is depicted in Fig. 5.

Kasowski identifies the peak at 0.9 eV for $\vec{E} \parallel \vec{c}$ as arising from transitions in the hexagonal (ΓMK) plane about $\frac{2}{3}$ of the distance to the zone face. In the band structure these transitions are seen along $\Gamma M(\Sigma_1 \rightarrow \Sigma_3)$ and $\Gamma K(T_4 \rightarrow T_2)$. Here, bands which are degenerate in the free-electron model are split by the crystal potential, resulting in nearly parallel bands which cross E_F and give rise to optical absorption. Electric dipole transitions are allowed along Σ and T for $\vec{E} \parallel \vec{c}$ only, and the calculated interband matrix elements are large. This assign-

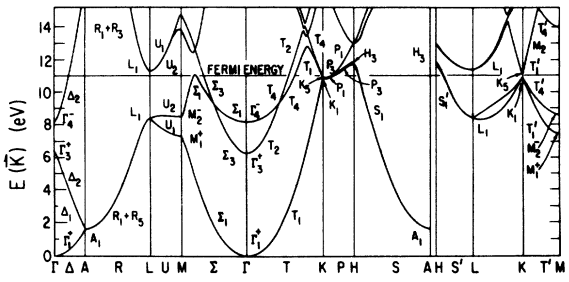

FIG. 4. Band structure of Zn from Stark and Falicov (Ref. 5).

ment and the calculated shape and position are in very good agreement with the present experimental results.

The broad double peak in ϵ_2/λ centered at 2.5 eV and occurring for both polarizations in the calculation is assigned by Kasowski to the $LH(S')$ region of the Brillouin-zone face, where again the bands are nearly parallel and oscillator strengths are large. Here, however, electric dipole transitions are allowed for both polarizations. These bands are also degenerate in the free-electron model and are split by the crystal potential. The doublet nature of this structure is attributed to the sharp change in curvature of the bands along LH near the L point. This theoretical doublet would agree with the present experimental observations if shifted to lower energy by 0.9 eV.

The preceding interpretation of the optical spectra gives good agreement between theory and experiment for the interband energy along ΓM and ΓK, but poor agreement for that along LH in the Brillouin zone. This difference in accuracy can result from the choice of the pseudopotential. Both structures arise from splitting of degenerate states by the crystal potential. This splitting is twice as large for the LH structure as for the ΓM-ΓK structure, so that a given inaccuracy in the pseudopotential should result in a larger error in the interband energy at LH than along ΓM and ΓK. Furthermore, precise knowledge of the Fermi-surface $\vec{k}$ vectors does not determine the slope of the bands at E_F. In fact, the same Fermi surface and a smaller slope of the lower bands along LH would reduce the interband separation along LH, improving agreement with experiment.[15]

Stark and Auluck[16] are presently attempting to improve the Zn pseudopotential to obtain a good fit of the band structure to the cyclotron-resonance data of Sabo[17] for the Zn third-band "lens." The cyclotron-resonance masses give a measure of the slope of the bands at E_F. Stark and Auluck indicate that the d potential must be decreased to fit the data of Sabo as well as the previous Fermi-surface data. This change in the nonlocal pseudopotential flattens the bands at E_F and reduces the interband energies along LH considerably more than it does the energies along ΓM and ΓK. Hence, better agreement with the optical spectra is to be expected.

The observed shift of the LH structure to lower energy with increasing temperature is expected: Phonons effectively smooth out the crystal potential as seen by the electrons, so that the splitting of the bands along LH caused by the crystal potential is reduced. This argument should hold for the ΓM-ΓK structure as well, but the observed temperature shift has the opposite sign. This surprising result may arise from the anisotropic thermal-expansion coefficient and deformation potentials or from the shift of the Fermi energy relative to the bands with temperature.

VII. MAGNITUDES AND SUM RULE

The magnitude of the ΓM-ΓK peak measured here corresponds roughly to the room-temperature result of GL and is about half the magnitude of the theoretical peak. For the LH structure, the present results agree with the GL results for $\vec{E} \perp \vec{c}$. The observed magnitude for $\vec{E} \perp \vec{c}$ is somewhat larger than that for $\vec{E} \parallel \vec{c}$. The difference is, however, not quite as large as in the theory, which attributes larger matrix elements to the perpendicular polarization.

An indication of the accuracy of the magnitudes of ϵ_2/λ is obtained from calculating the sum rule for ϵ_2:

$$\int_0^\infty \omega\epsilon_2(\omega)\, d\omega = \frac{2\pi^2 N n_{eff} e^2}{m_o} \quad , \tag{3}$$

where the right-hand side is just $\frac{1}{2}\pi\omega_p^2$, N is the atomic density of the crystal, and n_{eff} is the effective number of electrons per atom. We assume the sum rule (3) applies individually to the independent components $\epsilon^{\parallel}$ and $\epsilon^{\perp}$ of the second-rank dielectric tensor. For Zn, n_{eff} should saturate at $n_{eff} = 2.0$ when the oscillator strength of the two outer s electrons of the atoms is exhausted. Expressing (3) in terms of ϵ_2/λ,

$$n_{eff}(\hbar\omega) = \frac{m_o c}{\pi N e^2 \hbar} \int_0^{\hbar\omega} \frac{\epsilon_2}{\lambda}(\hbar\omega)\, d(\hbar\omega) \quad . \tag{4}$$

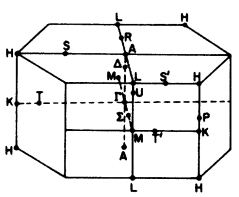

FIG. 5. First Brillouin zone of the hexagonal close-packed lattice.

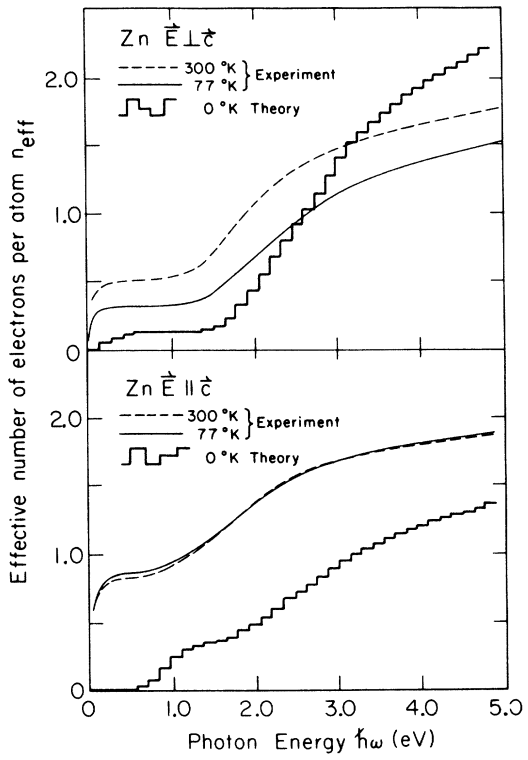

FIG. 6. Sum rules for Zn. Theory is calculated from the interband ϵ_2/λ values of Kasowski (Ref. 6).

Thus n_{eff} is proportional to the area under the curves in Fig. 3. This function is plotted up to 5 eV in Fig. 6. At 11.0 eV, just above the plasma energy for the two s electrons, the experimental n_{eff} is within 3% of 2.00 for all curves except $\vec{E}\perp\vec{c}$ at 77 °K, which has $n_{eff}=1.79$. The asymptotic approach to $n_{eff}=2.0$ implies that the average of ϵ_2/λ magnitudes over the whole spectrum is accurate to about ±10%. This indicates that the extrapolations made for Kramers-Kronig analysis and the resulting magnitudes of ϵ_2/λ are reasonable. However, the lower value of n_{eff} for $\vec{E}\perp\vec{c}$ at 77 °K suggests that the corresponding reflectance magnitudes are too small and that the decrease in reflectance for $\vec{E}\perp\vec{c}$ upon cooling from 300 °K is erroneous.

Since the theoretical spectra include only interband absorption, a contribution for intraband absorption must be added to compare with experiment. This can be estimated from the results of Kramers-Kronig analysis shown in Fig. 3. The intraband absorption appears to be mostly confined to $\hbar\omega \leq 0.5$ eV, and interband structure essentially begins above this energy. Thus n_{eff} (0.5 eV) is the estimated intraband contribution, which is about 0.85 for $\vec{E}\parallel\vec{c}$ and 0.5 for $\vec{E}\perp\vec{c}$. We have calculated n_{eff} from Kasowski's interband ϵ_2/λ and included it in Fig. 6. At 4.9 eV we find that $n_{eff}^{\parallel}=1.36$ and $n_{eff}^{\perp}=2.19$. Adding to this the estimated intraband contributions we obtain $n_{eff}^{\parallel}=2.2$ and $n_{eff}^{\perp}=2.7$ at only 4.9 eV. Thus the theory gives absorption magnitudes which are at least 10–20% too large in consideration of the requirements of the sum rule. If the magnitudes of the theoretical ϵ_2/λ curves are artificially adjusted to fit the sum rule more closely, both curves must be reduced, the perpendicular polarization more than the parallel. This brings the magnitudes into better agreement with the data obtained here by Kramers-Kronig analysis, but does not change the discrepancy in the relative heights of the 0.9-eV peak and 1.6-2.1-eV doublet observed for $\vec{E}\parallel\vec{c}$.

VIII. CONCLUSION

Previous experimental evidence suggests that the optical properties of Zn above 3.0 eV are primarily free-electron-like. Therefore a reasonable extrapolation of the reflectance can be made in order to obtain the optical constants by Kramers-Kronig analysis of normal incidence reflectance data. The validity of the extrapolation procedure and the accuracy of the resulting ϵ_2/λ spectra are given support by satisfaction of the sum rule for ϵ_2 and by the relative insensitivity of the interband structure in ϵ_2/λ to changes in the extrapolation parameters.

The theoretical optical spectra of Zn calculated from an empirical nonlocal pseudopotential band-structure fit to Fermi-surface data are in considerably better agreement with the present normal-incidence reflectance results than with previous oblique incidence data. The good agreement between theory and the present experiment for the shape and polarization dependence of interband structure suggests that the general features of this band structure are correct. In analyzing the optical spectra, we have assumed that direct transitions by single electrons dominate the interband absorption.

The theory correctly predicts the 0.9-eV energy of interband transitions along ΓM and ΓK in the interior of the Brillouin zone, but for transitions at the zone face along LH the calculated energies lie ≈0.9 eV above the measured energy range of 1.6–2.1 eV. Errors in the interband energies can arise from departures from the optimum pseudopotential coefficients. Recent calculations[16] indicate that (a) the Zn pseudopotential of SF does not give optimum agreement with available data describing the bands in the immediate vicinity of E_F; (b) fitting the band structure to cyclotron mass data in addition to other Fermi-surface data will improve the pseudopotential for bands near E_F; and (c) agreement with the measured optical spectra will improve as the pseudopotential is optimized. How-

ever, from the results now available, one cannot draw definite conclusions about the ultimate accuracy of the band structure obtained with the empirical nonlocal pseudopotential scheme for Zn.

The theoretical interband ϵ_2/λ spectra yield values of n_{eff} which are at least 10–20% too large to satisfy the sum rule. Hence, we conclude that the optical matrix elements calculated from the band structure are too large. This is not surprising because the main contribution to the interband n_{eff} comes from the doublet structure involving transitions along the LH line at the Brillouin face, where the calculated interband energy is too large and the bands are not accurately predicted by the theory. In addition, the theory gives a value of ϵ_2/λ for the 0.9-eV peak which is twice as large as the magnitude obtained from experiment.

Clearly, in order to predict the band structure of Zn away from E_F using an empirical pseudopotential band structure calibrated at E_F, a minimum requirement is the availability of precise data from several kinds of experiments, so that not only the position, but also a measure of the slope of several bands at E_f, is known. The agreement between experimental and theoretical shapes of the optical spectra is encouraging evidence that the empirical pseudopotential scheme is useful for Zn, but the present accuracy of the band structure away from E_F is not impressive. For the practical matter of depicting approximate band structures over a range of several eV, the accuracy and amount of data from experiments which probe electronic states at the Fermi surface may require a more difficult effort than the measurement of optical gaps and their consequent use in determining pseudopotential coefficients.

ACKNOWLEDGMENTS

The author wishes to thank H. Fritzsche and U. Gerhardt for their invaluable advice and assistance; R. V. Kasowski for his encouragement, cooperation, and stimulating discussion; F. Wooten, G. Dresselhaus, M. S. Dresselhaus, R. W. Stark, and S. Auluck for interesting discussions of this problem; and D. Dennison for suggestions and help in growing the crystals.

---

†Research sponsored by the Air Force Office of Scientific Research, Office of Aerospace Research, USAF. The U.S. Government is authorized to reproduce and distribute reprints for Governmental purposes notwithstanding any copyright notation hereon. We have also benefited from support of Materials Sciences by the Advanced Research Projects Agency at The University of Chicago.

*Submitted in partial fulfillment of the requirements for the Ph.D. degree at The University of Chicago.

‡Fannie and John Hertz Foundation Fellow.

[1]W. A. Harrison, *Pseudopotentials in the Theory of Metals* (Benjamin, New York, 1966).

[2]J. A. Appelbaum, Phys. Rev. 144, 435 (1966).

[3]H. Ehrenreich, H. Philipp, and B. Segall, Phys. Rev. 132, 1918 (1963).

[4]F. M. Mueller and J. C. Phillips, Phys. Rev. 157, 600 (1967).

[5]R. W. Stark and L. M. Falicov, Phys. Rev. Letters 19, 795 (1967).

[6]R. V. Kasowski, Phys. Rev. 187, 885 (1969).

[7]R. H. W. Graves and A. P. Lenham, J. Opt. Soc. Am. 58, 126 (1968).

[8]A. H. Lettington, in *Optical Properties and Electronic Structures of Metals and Alloys*, edited by F. Abeles (North-Holland, Amsterdam, 1966), p. 147.

[9]Recently an alternative computational technique has been developed [see, e.g., W. J. Scouler and P. M. Raccah, Bull. Am. Phys. Soc. 15, 289 (1970)], in which the dielectric function is represented by a sum of Lorentzian oscillators. Coefficients in the sum are determined by fitting the reflectance calculated from this dielectric function to the measured reflectance.

[10]U. Gerhardt and G. W. Rubloff, Appl. Opt. 8, 305 (1969).

[11]M. Kastner (private communication).

[12]L. P. Mosteller, T. Huen, and F. Wooten, Phys. Rev. 184, 364 (1969).

[13]L. P. Mosteller and F. Wooten, Phys. Rev. 171, 743 (1968).

[14]For $\vec{E} \perp \vec{c}$ the scale factor is 0.93 at 300 °K and 0.83 at 77 °K, while for $\vec{E} \parallel \vec{c}$ it is 0.99 at both temperatures.

[15]G. Dresselhaus and M. S. Dresselhaus (private communication).

[16]R. W. Stark and S. Auluck (private communication).

[17]J. J. Sabo, Jr., Phys. Rev. B 1, 1479 (1970).